ISSN 0036-0236, Russian Journal of Inorganic Chemistry, 2008, Vol. 53, No. 10, pp. 1566–1572. © Pleiades Publishing, Ltd., 2008.
Original Russian Text © A.S. Burlov, V.N. Ikorskii, S.A. Nikolaevskii, Yu.V. Koshchienko, V.G. Vlasenko, Ya.V. Zubavichus, A.I. Uraev, I.S. Vasil'chenko, D.A. Garnovskii, G.S. Borodkin, A.D. Garnovskiia, 2008, published in Zhurnal Neorganicheskoi Khimii, 2008, Vol. 53, No. 10, pp. 1677–1683.

New Ferro- and Antiferromagnetic Complexes of Tridentate Azomethines with Copper

A. S. Burlov[a], V. N. Ikorskii[b,†], S. A. Nikolaevskii[a], Yu. V. Koshchienko[a], V. G. Vlasenko[c], Ya. V. Zubavichus[d], A. I. Uraev[a], I. S. Vasil'chenko[a], D. A. Garnovskii[e], G. S. Borodkin[a], and A. D. Garnovskii[a]

[a] *Research Institute of Physical and Organic Chemistry, Southern Federal University, pr. Stachki 194/2, Rostov-on-Don, 344090 Russia*
[b] *International Tomography Center, Siberian Branch, Russian Academy of Sciences, ul. Institutskaya 3A, 630090 Novosibirsk, Russia*
[c] *Research Institute of Physics, Southern Federal University, pr. Stachki 194, Rostov-on-Don, 344090 Russia*
[d] *Kurchatov Institute Russian Research Center, pl. Kurchatova 1, Moscow, 123182 Russia*
[e] *Southern Scientific Center, Russian Academy of Sciences, ul. Chekhova 11, Rostov-on-Don, 344006 Russia*

Received September 10, 2007

Abstract—Tridentate azomethine ligands with N_2O_4 and N_3 donor atoms and their copper complexes were synthesized and characterized. The dimeric structure of copper(II) chelates was confirmed by EXAFS studies. Complexes based on 2-tosylaminobenzaldehyde azomethines tend to undergo ferromagnetic exchange, whereas similar salicylaldehyde derivatives have antiferromagnetic exchange.

DOI: 10.1134/S0036023608100082

As a development of studies dealing with targeted synthesis of ferro- and antiferromagnetic complexes of azomethine ligands [1–4], we synthesized for the first time the tridentate Schiff bases (**I**) with various aldehyde and amine fragments

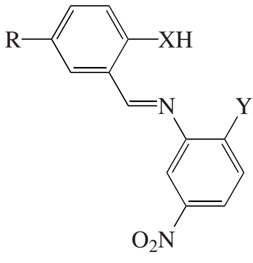

I

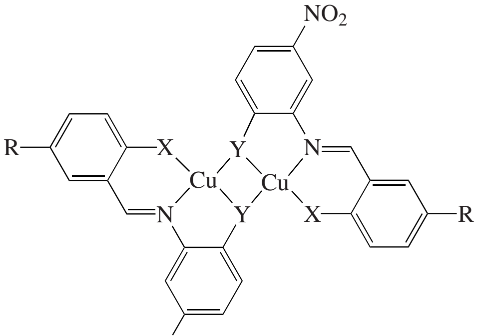

II X = NTs

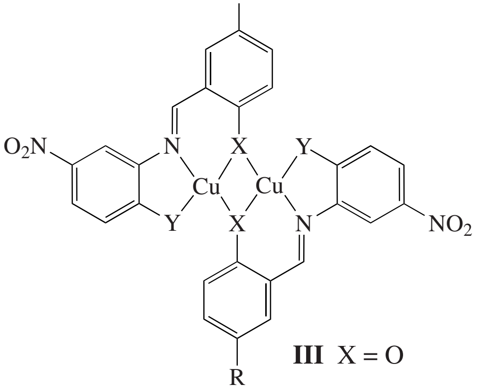

III X = O

X = NTs, Y = NCH_3, R = H (a);
X = NTs, Y = NC_2H_5, R = Br (b);
X = NTs, Y = NC_3H_7-*n*, R = H (c);
X = O, Y = $NPhCF_3$-*m*, R = H (d);
X = O, Y = NC_2H_5, R = Br (e);
X = O, Y = NC_3H_7-*n*, R = Me (f);
X = O, Y = NPh, R = H (g)

[†] Deceased

These compounds were used to prepare copper(II) complexes for which structures with different metal–metal bridges are possible (**II** and **III**).

EXPERIMENTAL

IR spectra were recorded on a Nicolet Impact 400 spectrophotometer for mineral oil mulls. ^{1}H NMR spectra were recorded in $CDCl_3$ on a Varian Unity-300 spectrometer (300 MHz) with the internal deuterium lock.

CuK-edge X-ray absorption spectra were recorded in the transmission mode on an EXAFS spectrometer at the structural materials science station of the Kurchatov Synchrotron Center (Moscow). The electron beam energy used as the X-ray synchrotron radiation source was 2.5 GeV at a current of 80–100 mA. A double-crystal Si(111) monochromator was used for X-ray monochromatization.

The spectra were processed by standard procedures including background removal, normalization to the K-edge jump, and subtraction of the atomic absorption μ_0 [5]. Then, the resulting EXAFS (χ) spectra were subjected to Fourier transform in the range of photoelectron wave vectors k from 2.6 to 12.6 Å^{-1} with the weight function k^3. The threshold ionization energy E_0 was chosen from the maximum of the first derivative of the K edge and was subsequently varied during fitting.

The exact values for the parameters of the local environment structure of copper atoms were found by nonlinear fitting of the parameters of corresponding coordination spheres by comparing the calculated EXAFS signal with that isolated from the full EXAFS spectrum by Fourier filtration. The nonlinear fitting was performed by using the IFFEFIT-1.2.5 software [6]. The phases and amplitudes of photoelectron wave scattering needed to simulate the spectrum were calculated with the FEFF7 software [7]. The single crystal X-ray diffraction data for $C_{22}H_{22}Cu_2N_2O_4$, acetylacetonemono(o-hydroxyanil)copper(II) dimer (ACHANC) [8], which are deposited at the Cambridge Crystallographic Data Centre [9], were taken as the initial atomic coordinates needed to calculate the scattering phases and amplitudes and for the subsequent fitting.

The quality of fit Q, which was minimized when determining the structure parameters of the local environment, was calculated by the formula

$$Q(\%) = \frac{\sum[k\chi_{\mathrm{exp}}(k) - k\chi_{\mathrm{theor}}(k)]^2}{\sum[k\chi_{\mathrm{exp}}(k)]^2} \cdot 100\%.$$

The magnetic measurements of the complexes were carried out on a Quantum Design SQUID magnetometer in the temperature range of 2–300 K in a 5-Oe magnetic field. In calculations of the paramagnetic component of the magnetic susceptibility χ, the additive diamagnetic contributions of ions were taken into account in conformity with the Pascal constants. The effective magnetic moment as a function of temperature was calculated as follows [10, 11]:

$$\mu_{\mathrm{eff}}(T) = \left(\frac{3k}{N\beta^2}\chi T\right)^{1/2} \approx (8\chi T)^{1/2},$$

where N, k, and β are the Avogadro number, the Boltzmann constant, and the Bohr magneton, respectively.

Synthesis of Anilines

2,4-Dinitro-*N*-methylaniline. Methylamine hydrochloride (7.43 g, 0.11 mol) was added to a suspension of 2,4-dinitrochlorobenzene (20.26 g, 0.1 mol) and $CH_3COONa \cdot 3H_2O$ (29.94 g, 0.22 mol) in ethanol (50 mL). The mixture was refluxed for 2 h and cooled, and the precipitate was filtered off and washed with water and ethanol. Yield, 14.98 g (76%); mp 178–179°C (from ethanol), which is consistent with the literature data [12].

2-Methylamino-5-nitroaniline. A suspension of N-methyl-2,4-dinitroaniline (19.71 g, 0.1 mol) in ethanol (40 mL) was added to a warm solution of $Na_2S \cdot 9H_2O$ (48.01 g, 0.2 mol) and crystalline sulfur (6.41, 0.2 mol) in water (63 mL). The mixture was refluxed for 2 h, diluted with water (30 mL), and cooled. The precipitate was filtered off and washed with warm water. Yield, 12.37 g (74%); dark red crystals, mp = 177°C (from ethanol), which is consistent with the literature data [13].

2,4-Dinitro-*N*-propylaniline. Propylamine (7.39 g, 0.125 mol) was added to a suspension of 2,4-dinitrochlorobenzene (20.26 g, 0.1 mol) and $CH_3COONa \cdot 3H_2O$ (29.94 g, 0.22 mol) in ethanol (40 mL). The mixture was refluxed for 4 h and cooled, and the precipitate was filtered off and washed with water and ethanol. Yield, 21.17 g (94%); yellow crystals, mp 95°C (from ethanol), which is consistent with the literature data [14].

2-Propylamino-5-nitroaniline was prepared similarly to 2-methylamino-5-nitroaniline except that the reaction mixture was refluxed for 4 h. Yield, 67%; dark red crystals, mp = 117–118°C (from benzene), which is consistent with the literature data [15].

2,4-Dinitro-*N*-(*m*-trifluoromethylphenyl)aniline was prepared similarly to 2,4-dinitro-N-propylaniline from 2,4-dinitrochlorobenzene and m-trifluoromethylaniline. Yield, 68%; yellow crystals, mp 123–124°C (from ethanol).

For $C_{13}H_8F_3N_3O_4$ anal. calcd. (%): C, 47.72; H, 2.46; N, 12.84.

Found (%): C, 47.66; H, 2.52; N, 12.90.

^{1}H NMR, δ, ppm: 7.18 (d, 1H, J^o = 9.5 Hz, C_{Ar}–H), 7.51–7.66 (m, 4H, C_{Ar}–H), 8.25 (dd, 1H, J^o = 9.5 Hz, J^m = 2.6 Hz, C_{Ar}–H), 9.20 (d, 1H, J^m = 2.6 Hz, C_{Ar}–H), 9.98 (br.s 1H, NH).

2-(*m*-Trifluoromethylphenyl)amino-5-nitroaniline was prepared similarly to 2-propylamino-5-nitroaniline.

Yield, 55%; dark red crystals, mp = 167–168°C (from ethanol).

For $C_{13}H_{10}F_3N_3O_2$ anal. calcd. (%): C, 52.53; H, 3.39; N, 14.14.

Found (%): C, 52.46; H, 3.45; N, 14.21.

^{1}H NMR, δ, ppm: 3.82 (br.s, 2H, NH_2), 5.79 (br.s, 1H, NH), 7.15–7.28 (m, 4H, C_{Ar}–H), 7.43 (t, 1H, J^o = 7.9 Hz, C_{Ar}–H), 7.69–7.73 (m, 2H, C_{Ar}–H).

2,4-Dinitro-*N*-phenylaniline. Freshly distilled aniline (10.25 g, 0.11 mol) was added to a suspension of 2,4-dinitrochlorobenzene (20.26 g, 0.1 mol) and $CH_3COONa \cdot 3H_2O$ (13.61 g, 0.1 mol) in ethanol (50 mL). The mixture was refluxed for 1 h and cooled, and the precipitated red-orange crystals were filtered off and washed with water and ethanol. Yield, 24.88 g (96%); mp = 156–157°C (from ethanol), which is consistent with the literature data [16].

2-Phenylamino-5-nitroaniline. A suspension of *N*-phenyl-2,4-dinitroaniline (25.92 g, 0.1 mol) in ethanol (60 mL) was added to a warm solution of $Na_2S \cdot 9H_2O$ (48.01 g, 0.2 mol) and crystalline sulfur (6.41, 0.2 mol) in water (60 mL). The mixture was refluxed for 2 h, diluted with water (30 mL), and cooled. The precipitate was filtered off and washed with warm water. Yield, 19.5 g (85%); dark brown crystals, mp = 125°C (from ethanol), which is consistent with the literature data [17].

Synthesis of Azomethines I

2-Tosylaminobenzaldehyde and 5-bromo-2-tosylaminobenzaldehyde were prepared by a known procedure [18].

Compounds Ia–Ig (general procedure). A solution of 2-methyl- (ethyl-, propyl-, phenyl-, *m*-trifluoromethyl)amino-5-nitroaniline (0.01 mol) in toluene (50 mL) was added to a solution of 2-tosylamino- or 5-bromo-2-tosylaminobenzaldehyde, salicylaldehyde, 5-bromo- or 5-methylsalicylaldehyde (0.01 mol) in toluene (30 mL), and the mixture was refluxed with a Dean–Stark trap under argon until water was completely removed (4 h). After completion of the reaction, the solvent was distilled off on a rotary evaporator to 1/4 of the initial volume. The precipitates formed after cooling were filtered off and recrystallized from an ethanol–chloroform mixture (2 : 1).

Ia. Yield 68%. Yellow-orange crystals, mp = 135–136°C.

For $C_{21}H_{20}N_4O_4S$ anal. calcd. (%): C, 59.42; H, 4.75; N, 13.20, S, 7.55.

Found (%): C, 59.55; H, 4.65; N, 13.83, S, 7.39.

^{1}H NMR, δ, ppm: 2.38 (s, 3H, NH–$\underline{CH_3}$), 3.08 (s, 3H, CH_3), 5.62 (s, 1H, $\underline{NH}$–CH_3), 6.61–8.21 (m, 11H, C_{Ar}–H), 8.68 (s, 1H, CH=N), 12.53 (s, 1H, NH). IR (cm^{-1}): 3640 (w, NH), 1620 (s, C=N), 1350 (vs, $\nu_{as}SO_2$), 1165 (vs, ν_sSO_2).

Ib. Yield 70%. Yellow-orange crystals, mp = 176–177°C.

For $C_{22}H_{21}BrN_4O_4S$ anal. calcd. (%): C, 51.07; H, 4.09; N, 10.83, S, 6.20.

Found (%): C, 51.27; H, 3.96; N, 11.02, S, 6.39.

^{1}H NMR, δ, ppm: 1.42 (t, 3H, ^3J = 7.1 Hz, CH_2–$\underline{CH_3}$), 2.37 (3H, c, CH_3), 3.39–3.43 (m, H, $\underline{CH_2}$–CH_3), 5.53 (t, 1H, ^3J = 4.9 Hz, $\underline{NH}$–C_2H_5), 6.67–8.17 (m, 11H, C_{Ar}–H), 8.65 (s, 1H, CH=N), 12.47 (s, 1H, NH). IR (cm^{-1}): 3640 (w, NH), 1620 (s, C=N), 1349 (vs, $\nu_{as}SO_2$), 1164 (o.c, ν_sSO_2), 1164 (vs, ν_sSO_2).

Ic. Yield 45%. Red-brown crystals, mp = 153–154°C.

For $C_{23}H_{24}BrN_4O_4S$ anal. calcd. (%): C, 61.05; H, 5.35; N, 12.38, S, 7.09.

Found (%): 61.16; H, 5.46; N, 12.64, S, 7.16.

^{1}H NMR, δ, ppm: 1.06 (t, 3H, ^3J = 7.4 Hz, CH_2–CH_2–$\underline{CH_3}$), 1.78–1.85 (m, 2H, ^3J = 7.4 Hz, CH_2–CH_2–$\underline{CH_3}$), 2.39 (s, 3H, CH_3), 3.30–3.37 (m, 2H, $\underline{CH_2}$–CH_2–CH_3), 5.54 (t, 1H, ^3J = 5.3 Hz, NH), 6.68 (d, 1 H, J^o = 9.2 Hz, C_{Ar}–H), 7.12–8.12 (m, 10H, C_{Ar}–H), 8.68 (s, 1H, CH=N), 12.44 (s, 1H, NH). IR (cm^{-1}): 3455 (w, NH), 1620 (s, C=N), 1351 (vs, $\nu_{as}SO_2$), 1165 (vs, ν_sSO_2).

Id. Yield 94%. Yellow crystals, mp = 179–180°C.

For $C_{20}H_{14}F_3N_3O_3$ anal. calcd. (%): C, 59.85; H, 3.52; N, 10.47.

Found (%): C, 60.01; H, 3.45; N, 10.56.

^{1}H NMR, δ, ppm: 6.81 (s, 1H, NH), 7.03–8.13 (m, 11H, C_{Ar}–H), 8.79 (s, 1H, CH=N), 11.48 (s, 1H, OH). IR (cm^{-1}): 3400 (w, NH), 1614 (s, C=N), 1276 (m, Ph–O).

Ie. Yield 73%. Orange crystals, mp = 182–183°C.

For $C_{15}H_{14}BrN_3O_3$ anal. calcd. (%): C, 49.47; H, 3.87; N, 11.54.

Found (%): C, 49.52; H, 3.89; N, 11.64.

^{1}H NMR, δ, ppm: 1.35 (t, 3H, ^{3}J = 7.2 Hz, CH_3), 3.31–3.40 (m, 2H, CH_2), 5.01 (s, 1H, NH), 6.65 (d, 1H, J^o = 9.1 Hz, C_{Ar}–H), 6.93–8.16 (m, 5H, C_{Ar}–H), 8.64 (s, 1H, CH=N), 12.32 (s, 1H, OH). IR (cm^{-1}): 3400 (w, NH), 1615 (s, C=N), 1277 (m, Ph–O).

If. Yield 65%. Brown crystals, mp = 160–161°C.

For $C_{17}H_{19}N_3O_3$ anal. calcd. (%): C, 65.16; H, 6.11; N, 13.41.

Found (%): C, 65.26; H, 6.15; N, 13.52.

^{1}H NMR, δ, ppm: 1.03 (t, 3H, ^3J = 7.3 Hz, CH_3), 1.72–1.77 (m, 2H, CH_2), 2.35 (s, 3H, CH_3), 3.27 (quint, 2H, ^3J = 6.6 Hz, CH_2), 5.17 (s, 1H, NH), 6.63 (d, 1H, J^o = 9.1 Hz, C_{Ar}–H), 6.93–8.14 (m, 5H, C_{Ar}–H), 8.64 (s, 1H, CH=N), 12.12 (s, 1H, OH). IR (cm^{-1}): 3400 (w, NH), 1615 (s, C=N), 1276 (m, Ph–O).

Ig. Yield 80%. Yellow needle crystals, mp = 206–207°C.

For $C_{19}H_{15}N_3O$ anal. calcd. (%): C, 68.46; H, 4.54; N, 12.61.

Found (%): C, 68.46; H, 4.54; N, 12.61.

^{1}H NMR, δ, ppm: 1.35 (t, 3H, ^3J = 7.2 Hz, CH_3), 3.31–3.40 (m, 2H, CH_2), 5.02 (s, H, NH), 6.65 (d, 1H, J^o = 9.1 Hz, C_{Ar}–H), 6.93–8.16 (m, 5H, C_{Ar}–H), 8.64 (s, 1H, CH=N), 12.32 (s, 1H, OH). IR (cm^{-1}): 3400 (w, NH), 1617 (s, C=N), 1276 (m, Ph–O).

Synthesis of Copper Complexes II

Compounds IIa–IIg (general procedure). A solution of copper acetate monohydrate (0.199 g, 0.001 mol) in ethanol (20 mL) was added to a solution of azomethine **Ia–g** (0.001 mol) in ethanol (50 mL). The mixture was refluxed for 4 h under argon. The finely crystalline precipitates of the complexes were filtered off, washed with boiling ethanol (3 × 5 mL), and dried in a vacuum drying chamber at 150°C.

IIa. Yield 75%. Red-brown powder, mp > 250°C.

For $C_{42}H_{36}N_8O_8S_2Cu_2$ anal. calcd. (%): C, 51.89; H, 3.73; N, 11.53; S, 6.60; Cu, 13.08.

Found (%): C, 51.92; H, 3.83; N, 11.64; S, 6.47; Cu, 13.21.

IR (cm^{-1}): 1603 (vs, C=N), 1285 (vs, $\nu_{as}SO_2$), 1138 (vs, ν_sSO_2).

IIb. Yield 83%. Brown powder, mp > 250°C.

For $C_{44}H_{38}Br_2N_8O_8S_2Cu_2$ anal. calcd. (%): C, 45.64; H, 3.31; N, 9.68; S, 5.54; Cu, 13.80.

Found (%): C, 45.78; H, 3.39; N, 9.62; S, 5.45; Cu, 13.92.

IR (cm^{-1}): 1604 (vs, C=N), 1283 (vs, $\nu_{as}SO_2$), 1137 (vs, ν_sSO_2).

IIc. Yield 65%. Brown powder, mp 233–234°C.

For $C_{46}H_{44}N_8O_8S_2Cu_2$ anal. calcd. (%): C, 53.74; H, 4.31; N, 10.90; S, 6.24; Cu, 12.36.

Found (%): C, 53.86; H, 4.46; N, 10.85; S, 6.35; Cu, 12.46.

IR (cm^{-1}): 1605 (s, C=N), 1285 (vs, $\nu_{as}SO_2$), 1135 (vs, ν_sSO_2).

IId. Yield 75%. Dark brown powder, mp > 250°C.

For $C_{40}H_{24}F_6N_6O_6S_2Cu_2$ anal. calcd. (%): C, 51.90; H, 2.61; N, 9.08; Cu, 13.73.

Found (%): C, 52.03; H, 2.57; N, 9.15; Cu, 13.92.

IR (cm^{-1}): 1602 (vs, C=N), 1327 (w, Ph–O).

IIe. Yield 72%. Brown powder, mp > 250°C.

For $C_{30}H_{24}Br_2N_6O_6Cu_2$ anal. calcd. (%): C, 42.32; H, 2.84; N, 9.87; Cu, 14.93.

Found (%): C, 42.38; H, 2.76; N, 9.91; Cu, 15.12.

IR (cm^{-1}): 1604 (s, C=N), 1328 (m, Ph–O).

IIf. Yield 80%. Red-brown powder, mp > 250°C.

For $C_{34}H_{34}N_6O_6Cu_2$ anal. calcd. (%): C, 54.46; H, 4.57; N, 11.21; Cu, 16.95.

Found (%): C, 54.58; H, 4.62; N, 11.32; Cu, 17.12.

IR (cm^{-1}): 1605 (s, C=N), 1330 (m, Ph–O).

IIg. Yield 81%. Brown powder, mp > 250°C.

For $C_{38}H_{26}N_6O_6Cu_2$ anal. calcd. (%): C, 57.79; H, 3.32; N, 10.64; Cu, 16.09.

Found (%): C, 57.82; H, 3.45; N, 10.72; Cu, 16.35.

RESULTS AND DISCUSSION

Complexes **II** and **III** were obtained by the direct reaction of ligand **I** (LH_2) with copper acetate monohydrate [19, 20]:

$$2LH_2 + Cu_2(CH_3COO)_4 \cdot 2H_2O \longrightarrow Cu_2L_2 + 4CH_3COOH + 2H_2O.$$

According to elemental analysis, complexes **II** have the composition M_2L_2. The chelate structure follows from analysis of their IR spectra. The C=N stretching frequency at 1600–1620 cm^{-1} decreases by 10–20 cm^{-1}, the $\nu_s(SO_2)$ and $\nu_{as}(SO_2)$ frequencies at 1350 and 1165 cm^{-1} decrease by 50 and 30 cm^{-1}, respectively, and the stretching bands for XH and YH acidic protons (3300–3450 cm^{-1}) disappear [21, 22].

The dimeric structure and the type of ligand environment are confirmed by analysis of the EXAFS spectra of complexes **II** (a, b, d, g).

Figure 1 shows the Fourier transform magnitudes (FTMs) of the Cu*K*-edge EXAFS spectra of **IIa**, **IIb**, **IId,** and **IIg**. All FTMs consist of two principal peaks with *r* of 2.39–2.40 Å and 2.39–2.40 Å, except for the FTM of **IId** where the second peak is shifted to greater distances and has the value *r* = 2.72 Å. The phases and amplitudes of photoelectron wave scattering were calculated proceeding from the model for the structure of these complexes in which two copper ions connected by two nitrogen bridges form bonds with two ligands (Cu–O and/or C–N). Multishell nonlinear of the simulated EXAFS spectrum to the experimental one gave parameters of the coordination sphere (table). As can be seen from the table, parameters of the first coordination sphere for all compounds do not differ much, indicating the same local environment of copper atoms in these compounds. The coordination number of copper in these complexes is four, the Cu–O and Cu–N distances and the Debye–Waller factor have typical values for this type of bonds. The second FTM peaks with greater distances are most likely due to short Cu–Cu distances. The results of nonlinear approximation made it possible to determine the quantitative characteristics of the second coordination sphere in the complexes. The Cu–Cu distances in **IIa**, **IIb,** and **IIg** (table) are in the range *R* = 2.70–2.85 Å; for **IId**, this distance is much longer (*R* = 3.02 Å).

Thus, EXAFS studies confirm the proposed dimeric structure of copper complexes **II** and **III**.

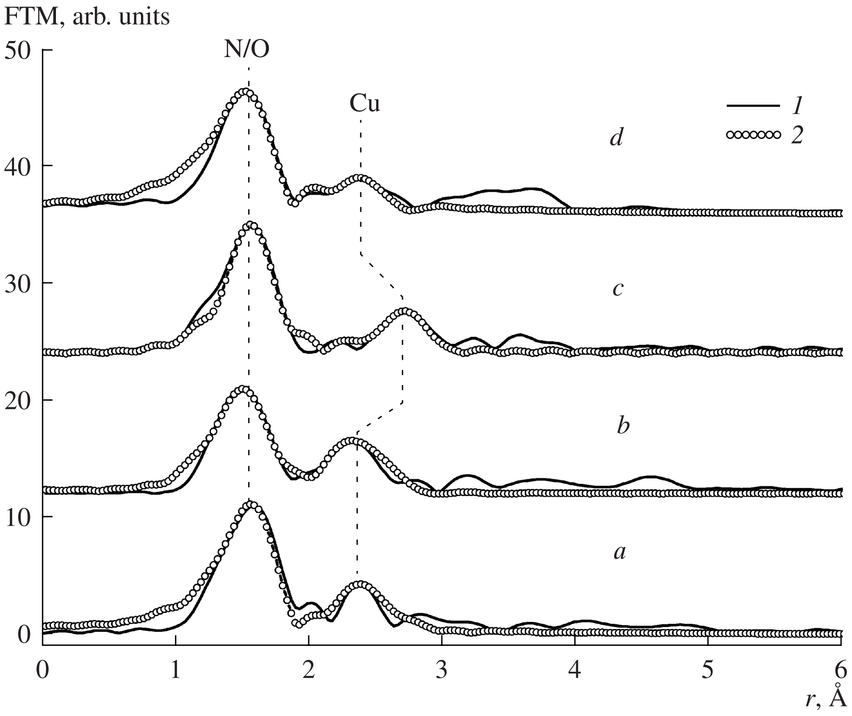

Fig. 1. FTM of the Cu*K*-edge X-ray EXAFS spectra for compounds (*a*) **IIa**, (*b*) **IIb**, (*c*) **IId**, (*d*) **IIg**. (*1*) Experimental FTMs and (*2*) simulated spectra.

The magnetochemical measurements for complexes **IIa**–**IIg** in the temperature range 300–2 K have shown (Figs. 2–8) that, for complexes **IIa**–**IIc** based on 2-tosylaminebenzaldehyde, ferromagnetic exchange coupling is typical (Figs. 2–4), whereas, in the coordination compounds of salicylaldehyde and its substituted derivatives, the exchange coupling is antiferromagnetic.

Structural data found from the multishell fitting of the EXAFS data (*R* are interatomic distances, *N* are the coordination numbers, σ^2 is the Debye–Waller factor, *Q* is the fitting quality function)

Compound	*N*	*R*, Å	σ^2, Å^2	Atom	*Q*, %
IIa	2	1.98	0.0051	N	
	2	2.07	0.0057	N	5.6
	1	2.84	0.0089	Cu	
IIb	4	1.90	0.0045		3.8
	1	2.70	0.0052	Cu	
IId	4	1.93	0.0028		4.2
	1	3.02	0.0035	Cu	
IIg	2	1.95	0.0034	N/O	
	2	2.03	0.0033	N/O	
	1	2.85	0.0092	Cu	6.0
	4	3.19	0.010	C	

This result may be attributed to the formation of structure **II** with Y = NAlk bridging fragments in the former case, whereas, in the latter case, oxygen metal–metal bridge **III** (Y = O) with a typical antiferromagnetic exchange coupling is formed [23].

The experimental $\mu_{\mathrm{eff}}(T)$ curves for complexes **II** (**III**) are presented in Figs. 2–8 (the solid lines show theoretical curves). Assuming a dimeric structure of the complexes, these dependences were theoretically simulated using the Bleaney–Bowers equation for the magnetic susceptibility of a dimer [10, 11]

$$\chi_{(\mathrm{Cu-Cu})} = \frac{N\beta^2 g^2}{3kT}\left[1 + \frac{1}{3}\exp\left(\frac{-2J}{kT}\right)\right]^{-1} + N\alpha$$

with inclusion of the exchange interaction between the dimers zJ'

$$\chi' = \frac{\chi_{(\mathrm{Cu-Cu})}}{(1 - (2zJ'/N\beta^2 g^2)\cdot\chi_{(\mathrm{Cu-Cu})})}$$

and a possible monomeric impurity *p* with the spin $S = 1/2$:

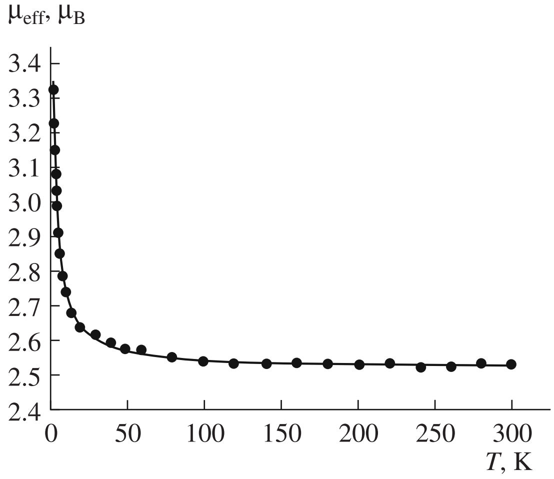

Fig. 2. Temperature dependence of the effective magnetic moment of **IIa**.

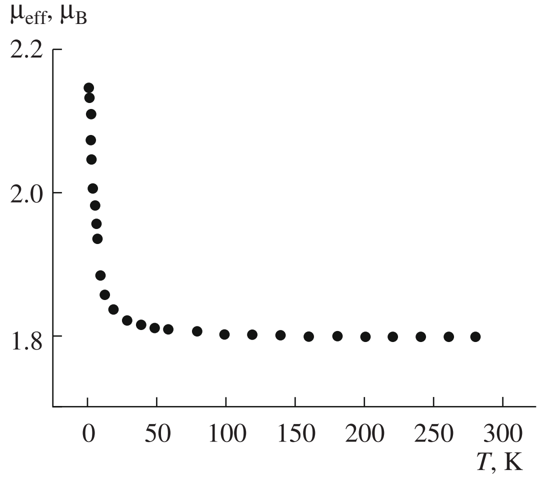

Fig. 3. Temperature dependence of the effective magnetic moment of **IIb**.

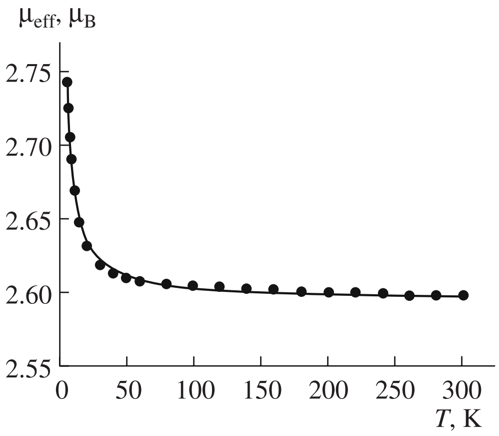

Fig. 4. Temperature dependence of the effective magnetic moment of **IIc**.

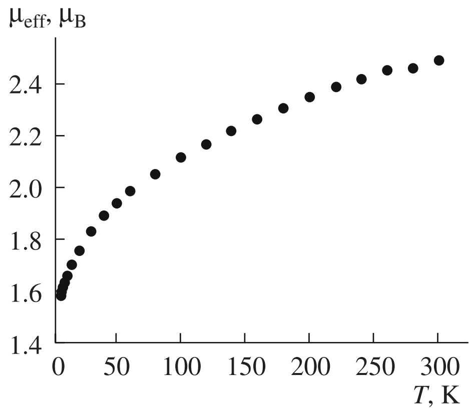

Fig. 5. Temperature dependence of the effective magnetic moment of **IId**.

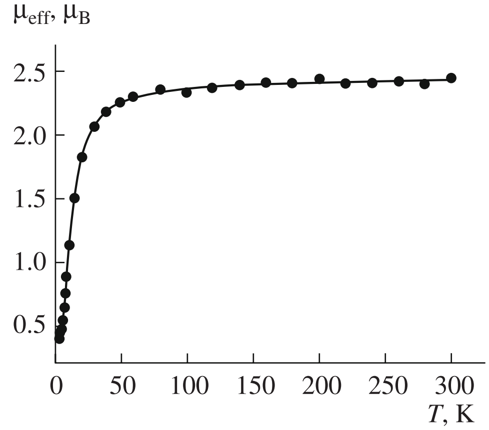

Fig. 6. Temperature dependence of the effective magnetic moment of **IIe**.

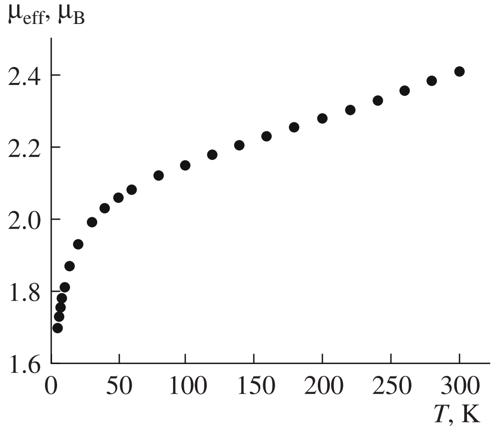

Fig. 7. Temperature dependence of the effective magnetic moment of **IIf**.

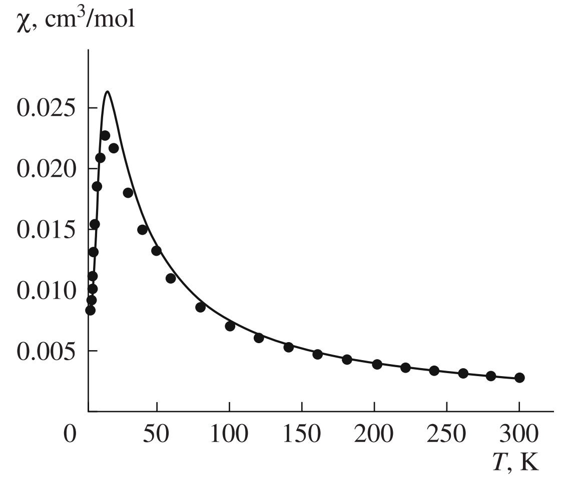

Fig. 8. Temperature dependence of the magnetic susceptibility of **IIg**.

$$\chi = \chi'(1-p) + \frac{N\beta^2 g^2 S(S+1)}{3k(T-\theta)}p.$$

Here N, $N\alpha$, k, β, J, g, and θ are the Avogadro number, van Vleck paramagnetism, the Boltzmann constant, the Bohr magneton, the exchange coupling parameter, the Lande factor, and the Weiss constant, respectively.

Thus, a change in the nature of the bridging fragment (X, Y) gives rise to dimeric copper complexes with different types of magnetic exchange: ferromagnetic (X = NTs) and antiferromagnetic (X = O) types.

ACKNOWLEDGMENTS

This work was supported by the Program of the Ministry of Science and Education of the Russian Federation “Development of the Scientific Potential” (2006–2008) (RNP.2.1.1.1875), by the Program of Presidium of the Russian Academy of Sciences (project “Molecular Design of Magnetically Active Compounds and Materials (Molecular Magnets)”), the Council for Grants of the President of the Russian Federation for State Support of Leading Scientific Schools (grant no. NSh-363.2008.3), and a Southern Federal University domestic grant.

REFERENCES

1. A. I. Uraev, I. S. Vasilchenko, V. N. Ikorskii, et al., Mendeleev Commun. **15** (4), 133 (2005).
2. A. S. Burlov, Yu. V. Koshchienko, V. N. Ikorskii, et al., Zh. Neorg. Khim. **51** (7), 1143 (2006) [Russ. J. Inorg. Chem. **51** (7), 1065 (2006)].
3. A. S. Burlov, V. N. Ikorskii, A. I. Uraev, et al., Zh. Obshch. Khim. **76** (8), 1337 (2006).
4. A. D. Garnovskii, V. N. Ikorskii, A. I. Uraev, et al., J. Coord. Chem. **60** (14), 1493 (2007).
5. D. I. Kochubei, Yu. A. Babanov, K. I. Zamaraev, et al., *X-ray Spectral Method of Investigation of the Structure of Amorphous Solids: EXAFS Spectroscopy* (Nauka, SO, Novosibirsk, 1988) [in Russian].
6. M. Newville, J. Synchrotron Rad., No. 8, 96 (2001).
7. S. I. Zabinski, J. J. Rehr, A. Ankudinov, and R. C. Alber, Phys. Rev. B: Condens, Matter **52**, 2995 (1995).
8. G. A. Barclay and B. F. Hoskins, J. Chem. Soc., 1979 (1965).
9. F. H. Allen, Acta Crystallogr. Sect. B: Struct. Sci. **58**, 380 (2002).
10. O. Kahn, *Molecular Magnetism* (Verlag-Chemistry, New York, 1993).
11. V. T. Kalinnikov and Yu. V. Rakitin, *Introduction to Magnetochemistry. The Static Magnetic Susceptibility Method* (Nauka, Moscow, 1980) [in Russian].
12. A. N. Lomakin, A. M. Simonov, and V. A. Chigrina, Zh. Obshch. Khim. **33** (1), 204 (1963).
13. B. A. Porai-Koshits and Ch. Frankovskii, Zh. Obshch. Khim. **28** (4), 928 (1958).
14. H. Brauniger and K. Spangenberg, Pharmazie **12**, 335 (1957).
15. C. Runti, Ann. Chim. (Rome) **46**, 406 (1956).
16. A. M. Simonov and V. A. Izmail’skii, Zh. Obshch. Khim. **16** (10), 1667 (1946).
17. R. Nietzki and K. Almenzader, Ber. Dtsch. Chem. Ges. **28** (15), 2969 (1895).
18. N. I. Chernova, Yu. S. Ryabokobylko, V. G. Brudz’, and B. M. Bolotin, Zh. Org. Khim. **7** (8), 1680 (1971).
19. A. D. Garnovskii, I. S. Vasil’chenko, and D. A. Garnovskii, *Modern Aspects of Synthesis of Metal Complexes. Ligands and Methods* (LaPO, Rostov-on-Don, 2000) [in Russian].
20. *Synthetic Coordination and Organometallic Chemistry*, Ed. by A. D. Garnovskii and B. I. Kharisov (Marcel Dekker, New York, 2003).
21. A. D. Garnovskii, V. A. Alekseenko, V. A. Kogan, et al., Koord. Khim. **3** (4), 500 (1977).
22. K. Nakamoto, *Infrared and Raman Spectra of Inorganic and Coordination Compounds*, 5th ed., part B (John Wiley, London, 1997).
23. V. A. Kogan and V. V. Lukov, Koord. Khim. **30** (3), 219 (2004).